



HAL
open science

New sulfonated perylene diimide pyrazolate ligands: a simple route toward n-type redox-active hybrid materials

Vincent Monnier, Fabrice Odobel, Stéphane Diring

► To cite this version:

Vincent Monnier, Fabrice Odobel, Stéphane Diring. New sulfonated perylene diimide pyrazolate ligands: a simple route toward n-type redox-active hybrid materials. *Chemical Communications*, 2022, 58 (67), pp.9429-9432. 10.1039/D2CC02427F . hal-03827891

HAL Id: hal-03827891

<https://hal.science/hal-03827891>

Submitted on 24 Oct 2022

HAL is a multi-disciplinary open access archive for the deposit and dissemination of scientific research documents, whether they are published or not. The documents may come from teaching and research institutions in France or abroad, or from public or private research centers.

L'archive ouverte pluridisciplinaire **HAL**, est destinée au dépôt et à la diffusion de documents scientifiques de niveau recherche, publiés ou non, émanant des établissements d'enseignement et de recherche français ou étrangers, des laboratoires publics ou privés.

COMMUNICATION

New sulfonated perylene diimide pyrazolate ligands: a simple route toward *n*-type redox-active hybrid materials

Vincent Monnier,^{*a} Fabrice Odobel^a and Stéphane Diring^{*a}

Received 00th January 20xx,
Accepted 00th January 20xx

DOI: 10.1039/x0xx00000x

We report the synthesis and the in depth electrochemical study of two novel electron accepting sulfonated perylene diimide pyrazolate ligands. Bridging the sulfone moieties of the perylene core, unexpectedly affected the optical and electronic properties as evidenced by spectroelectrochemical investigation. Notably, we achieved a significant lowering of the LUMO level to -4.83 eV, ranking the ligand among the best electron acceptors via a straightforward synthetic procedure. These ligands can be foreseen for the development of *n*-type functional materials.

Perylene diimides (PDIs) are electrodeficient fluorescent dyes that have been triggering interest for many applications, ranging from anion binding and sensing¹³ to anion- π catalysis,¹⁴ non-fullerene acceptor based organic photovoltaics^{15,16} or *n*-type organic field-effect transistors.^{17,18} PDIs combine attractive features such as low cost, strong light absorption, high emission quantum yields, excellent photochemical and electrochemical stabilities but also intrinsically low lying LUMO level.¹⁹ While the pristine unsubstituted PDI LUMO level lies at *c.a.* -4.20 eV,¹⁴ there is a huge interest in tuning this level, aiming particularly to achieve the lowest possible energy¹⁹ in order to strengthen application-relevant properties such as their quadrupole moment Q_{zz} for anion- π interaction. As every arylene diimides, PDIs can undergo two reduction events yielding to unusually stable radical anion $\text{PDI}^{\bullet-}$ and dianion PDI^{2-} , even in water for the later.²⁰ Lowering of the LUMO level with the introduction of electron withdrawing substituents on the aromatic core eases the formation and concomitantly stabilizes such reduced species.^{21,22} Such materials can be appealing when considering applications such as *n*-type electrochromism, faradic charge accumulation or multi-electronic oxidative catalysis.^{23,24}

From a design point of view, PDIs present a wide range of possibilities of substitution on the 8 positions of the π -conjugated core, while the imide N-substituents allow to introduce versatile functionalities with a minimal impact on the electronic properties of the dye.²⁸ This feature has been extensively explored, for instance to

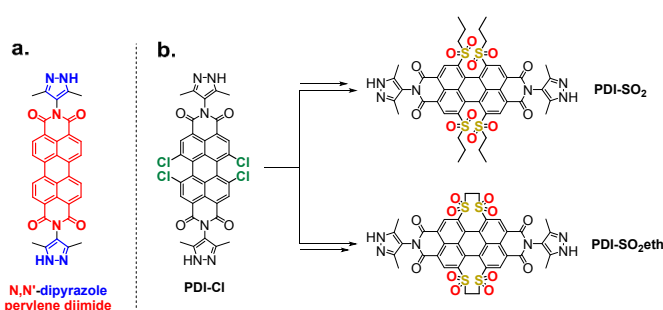


Fig. 1 (a.) Archetype *N,N'*-dipyrazole perylene diimide considered in this work and (b.) designed low-lying LUMO ligands.

tune the aggregation properties in assemblies relying on π -stacking,^{25,33} to introduce monomers toward organic functional polymers^{34,35} or various coordination functions for the elaboration of metal-organic hybrid materials.^{26,27,36} However, the introduction of extremely electrodeficient PDIs in such hybrid assemblies has not been realized so far, most likely due to their challenging synthesis which often requires harsh conditions and rely on inert *N*-substituents on the imide part that will remain resilient towards the chemical steps performed on the perylene core.¹⁹ Hence, providing new PDIs with both very low lying LUMO and coordination functions is a relevant purpose. To be consistent with the field of applications aimed for such deficient PDI, the choice of coordination function must lead to materials that remain stable even in electron rich media. Pyrazoles moieties are appealing as their coordination to various *d*-block metal ions (*e.g.*, Cu, Fe, Co, Zn) is well-studied and known to result in chemically stable hybrid materials, even in basic aqueous media.³⁷

Considering the aromatic PDI core, it has been shown that *bay* substitution with sulfones lead to low-lying LUMO levels on naphthalene diimide (NDI) analogues that are stable, notably in presence of water.³¹ Here, we have designed two new ligands, derived from the chlorinated parent PDI-Cl **4**³² (Figure 1), and bearing bay substituted sulfones with either open *n*-alkyl chain (PDI-SO₂) or closed ethylene bridges (PDI-SO₂eth **10**). Notably, we found that bridging the neighboring sulfone groups of a given *bay* region

^a Université de Nantes CEISAM UMR CNRS 6230, Nantes F-44000, France

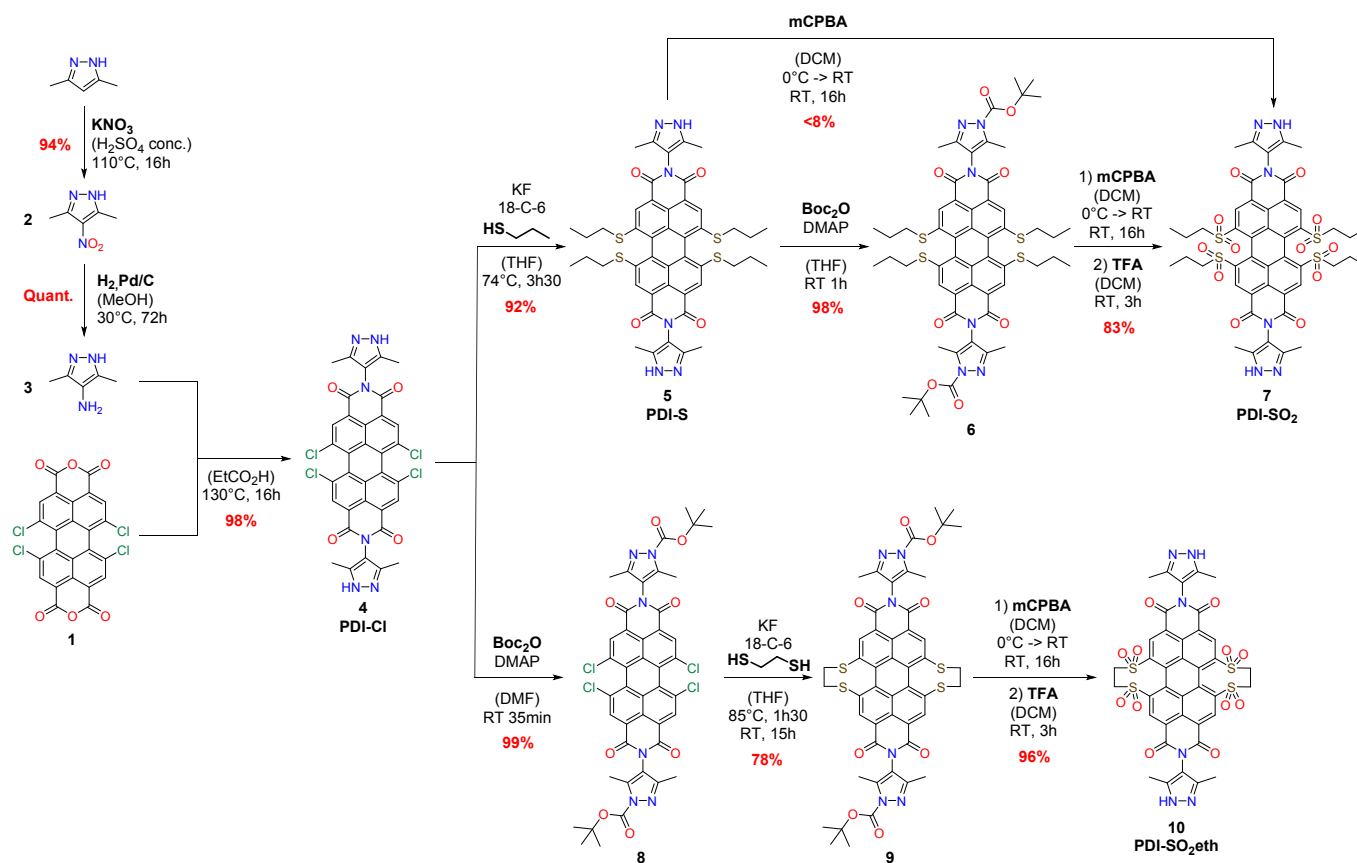


Fig. 2 Synthesis of the sulfonated bPDI ligands bPDI-SO₂ **7** and bPDI-SO₂eth **10**.

significantly impacted the electronic properties of the PDI dye and led to an extremely electrodeficient core, with a LUMO level standing amongst the lowest ones reported to date. The synthesis of the desired PDI ligands **4**, **7** and **10** is depicted in **Figure 2**. The 1,6,7,12-tetrachloro-perylene-3,4,9,10-tetracarboxylic dianhydride (PDA-Cl) **1** was obtained *via* a previously reported route.²¹ Briefly, chlorination of commercially available perylene-

3,4,9,10-tetracarboxylic dianhydride by chlorosulfonic acid, followed by esterification allowing purification and subsequent hydrolysis of the esters afforded pure PDA-Cl **1**. 5-nitro-3,5-dimethylpyrazole **2** was obtained by nitration of commercially available 3,5-dimethylpyrazole, and then efficiently reduced in 5-amino-3,5-dimethylpyrazole **3** by hydrogenation in presence of palladium on carbon. Further condensation of the pyrazole **3** on PDA-Cl **1** followed by *in-situ* high temperature dehydration produced the 1,6,7,12-tetrachloro-perylene-3,4,10,11-tetracarboxylic diimide PDI-Cl **4**. The route toward the sulfonated derivatives was inspired from the previously reported work of Fernandez-Lazaro *et al.*, who demonstrated efficient radical *bay*-substitution of halogens by thiols in presence of activated fluorides.²² The PDI-S **5** was hence obtained and subsequent complete sulfide oxidation with *meta*-chloroperoxybenzoic acid allowed to reach PDI-SO₂ **7**. Note that this oxidation cannot be efficiently performed without protection of the pyrazole moieties (*vide supra*, compound **6**), due to a fast degradation of the starting material upon exposure to oxidant. The same strategy was applied to prepare compound PDA-SO₂eth **10**, but the *tert*-butoxycarbonyl (Boc) moieties were introduced directly

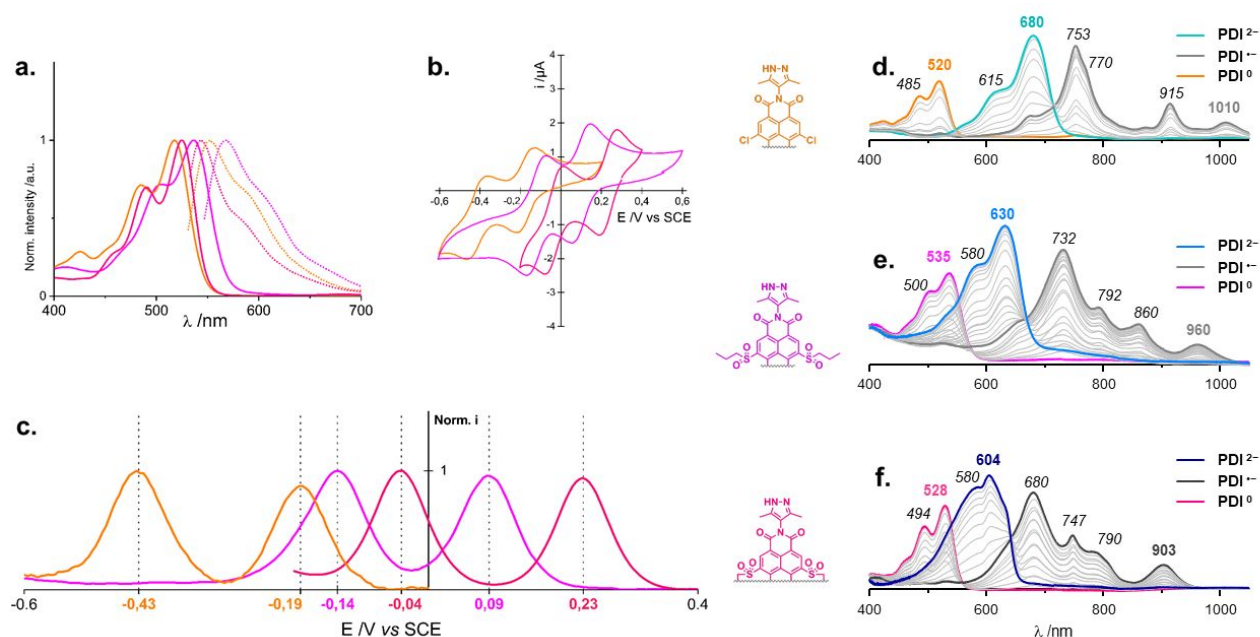
onto PDI-Cl **4**, in order to enhance solubility and thus both ease purification and enhance the rate of reaction.

The photophysical characteristics of the electrodeficient ligands PDI-Cl, PDI-SO₂ and PDI-SO₂eth were studied using UV/vis absorption and photoluminescence spectroscopy. No luminescence could be observed from any of these ligands under neutral pH conditions. However, acidification of the medium allowed for a strong fluorescence to be detected (**Figure S1**). Interestingly, luminescence was also observable for the Boc-protected derivative **8**. A short discussion on this matter is given in the Supplementary Information (see **Figure S2**).

The absorption-emission spectra recorded in acidified THF (9:1 THF/HCl aq. 2M) express the classical vibronic band structure of this type of perylene diimide, *bay*-substituted by electron-withdrawing groups (see **Figure 3a**, **Table 1**). The absence of donating groups on the perylene core leads inevitably to the absence of partial charge-transfer (CT) character and thus to purely core-centered π - π^* transitions. The intersection of the normalized absorption and emission spectra allowed an estimation of the first excited state energy, identical for PDI-Cl and PDI-SO₂eth ($E_{0-0} = 2,32$ eV) and inferior for PDI-SO₂ ($E_{0-0} = 2,25$ eV).

The electrochemical characterization of the ligands was performed in 0,1M TBAPF₆ DMF solution. Reversible cyclic voltammograms indicated good stability of the ligands toward reduction (see **Figure 3b**). In addition, comproportionation constants (K_c) were determined by equation (1):

$$K_c = e^{\left(\frac{nF\Delta E_{DPV}}{RT}\right)} \quad (1)$$



Where ΔE_{DPV} is the difference between the first and second reduction events, as extracted from the differential pulse voltammetry experiments. The obtained values point out the high stability of the radicals toward disproportionation (see Figure 3c, Table S1). The comproportionation constant for **PDI-SO₂eth** ($K_c = 3,7 \times 10^4$) is higher than for **PDI-SO₂** ($K_c = 5,2 \times 10^3$), indicating the impact of the *S*-substituents *i.e.*, propyl or ethylene bridge, regarding disproportionation reaction.

Fig. 3 (a.) UV-vis absorption (plain line) and emission (dotted line) normalized spectra, (b.) cyclic voltammograms and (c.) differential pulse voltammograms of bPDI-Cl (orange), bPDI-SO₂ (pink) and bPDI-SO₂eth (red). UV-vis-NIR absorption spectra resulting of the spectroelectrochemical measurements for (d.) bPDI-Cl, (e.) bPDI-SO₂ and (f.) bPDI-SO₂eth

reduction events, as extracted from the differential pulse voltammetry experiments. The obtained values point out the high stability of the radicals toward disproportionation (see Figure 3c, Table S1). The comproportionation constant for **PDI-SO₂eth** ($K_c = 3,7 \times 10^4$) is higher than for **PDI-SO₂** ($K_c = 5,2 \times 10^3$), indicating the impact of the *S*-substituents *i.e.*, propyl or ethylene bridge, regarding disproportionation reaction.

The first and second reduction potentials of **PDI-Cl** are $E_{DPV}(PDI^0/PDI^{\cdot-}) = -0,19$ V vs. SCE and $E_{DPV}(PDI^{\cdot-}/PDI^{2-}) = -0,41$ V vs. SCE, respectively. Following a predictable tendency, the corresponding potentials of **PDI-SO₂** are anodically shifted by $\Delta E_{DPV}(PDI^0/PDI^{\cdot-}) = +200$ mV and $\Delta E_{DPV}(PDI^{\cdot-}/PDI^{2-}) = +280$ mV. Surprisingly, the measured potentials of first and second reductions of **PDI-SO₂eth** are even more anodically shifted by +340 mV and +370 mV in regard of **PDI-Cl**, respectively. Such a noticeable difference most evidently arise from the bridging ethylene substituents. Moreover, the computed difference in energy between the semi-occupied molecular orbitals (SOMOs) of **PDI-SO₂^{•-}** radical and **PDI-SO₂eth^{•-}** radical $\Delta E_{SOMO} = +0,110$ eV is in good agreement with the observed difference $\Delta E_{DPV}(PDI/PDI^{\cdot-}) = +0,140$ V. However, computations did not evidence any readily rationalizable link between the structural impact of an ethylene bridge and the increase of electrodeficiency. Nevertheless, slight differences between both forms of bay-sulfonated PDI can be observed. For instance, bridged substituents constrain the π -conjugated backbone, resulting in an increase of the twist between the two naphthyl moieties, from 34.8° to 36.0°. Additionally, the oxygen atoms of the sulfones in **PDI-SO₂eth** are forced to point away from their closest naphthyl moiety,

which is not the case for **PDI-SO₂** (see Figure S5b). This restriction of orientation might be responsible for the observed experimental differences. In this idea, the computed repartition of the electron spin density for the radical reveal that, while the main part of the density difference remains unchanged on the π -conjugated core, a noticeable part of the oxygen atoms of the sulfones now contribute to accommodate the additional electron density (see Figure S5c).

	PDI-Cl	PDI-SO₂	PDI-SO₂eth
$\lambda_{abs} / \text{nm}$ (a)	518	536	525
$\lambda_{lum} / \text{nm}$ (a)	553	568	544
$\Delta\nu_{Stokes} / \text{cm}^{-1}$ (a)	1222	1051	665
E_{opt} / eV (a)	2.27	2.18	2.26
E_{0-0} / eV (a)	2.32	2.25	2.32
$\epsilon / \text{L} \cdot \text{mol}^{-1} \cdot \text{cm}^{-1}$ (a)	34850	26500	26100
$E_{1/2}(PDI/PDI^{\cdot-}) / \text{V vs SCE}$ (b)	-0.19	0.09	0.23
$E_{1/2}(PDI^{\cdot-}/PDI^{2-}) / \text{V vs SCE}$ (b)	-0.41	-0.13	-0.04
$E_{1/2}(PDI^{\cdot-}/PDI^{\cdot-}) / \text{V vs NHE}$	2.37	2.58	2.80

Table 1 : Summary of the main photophysical and electrochemical properties of the ligands **4 PDI-Cl**, **7 PDI-SO₂**, **10 PDI-SO₂eth**. (a) optical properties measured in THF/HCl aq. 9:1 solutions. (b) electrochemical properties measured in DMF TBAPF₆ 0.1M solutions. (c) Approximated LUMO values determined by taking -5.1 eV as the ferrocene value.

By means of relevant comparison with the literature,⁷ LUMO energies of the different ligands were approximated from the differential pulse voltammetry experiments, with a measured potential of the ferrocenium/ferrocene couple $E_{DPV}(Fc^+/Fc) = +0,5$ V

vs SCE in this system and by assuming -5.1 eV for Fc^+/Fc (see Table 1). The LUMO value $E_{LUMO} = -4.83$ eV of the **PDI-SO₂eth** ligand ranks it among the PDI electron acceptors having the lowest lying LUMO, readily accessible with a non-tedious pathway. Additionally, the reduced species of PDI-SO₂ and PDI-SO₂Et have been obtained chemically. UV-Vis absorption experiments have highlighted the excellent stability of the associated anionic radical and dianionic species under ambient conditions (see Figures S3 and S4). It is worth mentioning that by using an alkyl chain as the N-substituent and starting from **PDA-Cl**, one can reach such performant di-electron acceptor in three simple steps, namely imidation, nucleophilic aromatic substitution and sulfide oxidation.

Perylene diimide dyes being known for their electrochromicity,^{11,23} the n-type electrochromic properties of **PDI-Cl**, **PDI-SO₂** and **PDI-SO₂eth** were studied by spectroelectrochemical measurement in 0.1M TBAPF₆ DMF solution (see Figure 3d–f). Hence, upon application of a suited reductive potential, bathochromically shifted absorption bands appear, notably a broad signal in the NIR region for every PDI ($\lambda_{max} = 1010$ nm, 960 nm and 903 nm for **PDI-Cl**, **PDI-SO₂** and **PDI-SO₂eth**, respectively). This band is commonly attributed to D₀–D₁ transitions of PDI^{•-} specie. Further reduction to the dianion PDI²⁻ results in the appearance of hypsochromically shifted intense transitions in the visible region. The lowest energy bands, happening to be also the most intense, is this time associated with the S₀–S₁ transition ($\lambda = 680$ nm, 630 nm and 604 nm for **PDI-Cl**, **PDI-SO₂** and **PDI-SO₂eth**, respectively). As evidenced by the spectra in figure 3, whereas the UV/vis spectra are quite similar for every PDI in the neutral state, they present noteworthy differences in the reduced states PDI^{•-} and PDI²⁻. Specifically, the increasingly hypsochromic shifts are observed, resulting in the trend $\lambda_{abs}(PDI-Cl) > \lambda_{abs}(PDI-SO_2) > \lambda_{abs}(PDI-SO_2eth)$. This can be understood through the stabilization of the anions ground states (and thus newly occupied MO) consistent with the anodic shift of the reduction potentials. The counter-intuitive impact of the ethylene bridged substitution is here underlined once more by hypsochromic shifts of absorption as high as $\Delta\lambda_{abs} = 57$ nm and $\Delta\lambda_{abs} = 26$ nm when changing from PDI-SO₂^{•-} to PDI-SO₂eth^{•-} and from PDI-SO₂²⁻ to PDI-SO₂eth²⁻, respectively.

In conclusion, we report herein the simple and efficient synthesis of two new bay-sulfonated PDI pyrazolate ligands. These were fully characterized and present promising properties, exhibiting excellent electrochemical stability and among the lowest-lying LUMO levels reported for PDI. In the context of PDI as electron acceptor, we evidenced that an apparently innocent structural change such as substituting propyl chains for ethylene bridges had a significant impact on its electro-deficiency. This modification also imparts a reduced bulkiness of the ligand, which is desirable for the elaboration of highly porous hybrid n-type functional materials. MOF thin films based on these ligands and their electrochemical properties are in the course of being reported by our team.

Finally, ethylene-bridged sulfone appear as a promising substituent to aim for readily accessible stable low-lying LUMO PDI, whether the N-substituent is designed to be a coordination function or a simple alkyl chain.

Conflicts of interest

There are no conflicts to declare.

Notes and references

- K. Kumar, S. Kaur, S. Kaur, G. Bhargava, S. Kumar and P. Singh, *J. Mater. Chem. B*, 2020, **8**, 125–135.
- Y. Zhao, C. Beuchat, Y. Domoto, J. Gajewy, A. Wilson, J. Mareda, N. Sakai and S. Matile, *J. Am. Chem. Soc.*, 2014, **136**, 2101–2111.
- A. D. Hendsbee, J.-P. Sun, W. K. Law, H. Yan, I. G. Hill, D. M. Spasyuk and G. C. Welch, *Chem. Mater.*, 2016, **28**, 7098–7109.
- A. Nowak-Król, K. Shoyama, M. Stolte and F. Würthner, *Chem. Commun.*, 2018, **54**, 13763–13772.
- R. T. Weitz, K. Amsharov, U. Zscheschang, E. B. Villas, D. K. Goswami, M. Burghard, H. Dosch, M. Jansen, K. Kern and H. Klauk, *J. Am. Chem. Soc.*, 2008, **130**, 4637–4645.
- F. Würthner and M. Stolte, *Chem. Commun.*, 2011, **47**, 5109.
- S. Kumar, J. Shukla, Y. Kumar and P. Mukhopadhyay, *Org. Chem. Front.*, 2018, **5**, 2254–2276.
- M. A. Iron, R. Cohen and B. Rybtchinski, *J. Phys. Chem. A*, 2011, **115**, 2047–2056.
- S. Kumar and P. Mukhopadhyay, 26.
- S. Seifert, D. Schmidt and F. Würthner, *Chem. Sci.*, 2015, **6**, 1663–1667.
- W. Ma, L. Qin, Y. Gao, W. Zhang, Z. Xie, B. Yang, L. Liu and Y. Ma, *Chem. Commun.*, 2016, **52**, 13600–13603.
- J. T. Kirner, J. J. Stracke, B. A. Gregg and R. G. Finke, *ACS Appl. Mater. Interfaces*, 2014, **11**.
- F. Würthner, C. R. Saha-Möller, B. Fimmel, S. Ogi, P. Leowanawat and D. Schmidt, *Chem. Rev.*, 2016, **116**, 962–1052.
- B. Lü, Y. Chen, P. Li, B. Wang, K. Müllen and M. Yin, *Nat. Commun.*, 2019, **10**, 767.
- H. J. Park, M. C. So, D. Gosztola, G. P. Wiederrecht, J. D. Emery, A. B. F. Martinson, S. Er, C. E. Wilmer, N. A. Vermeulen, A. Aspuru-Guzik, J. F. Stoddart, O. K. Farha and J. T. Hupp, *ACS Appl. Mater. Interfaces*, 2016, **8**, 24983–24988.
- F. Würthner, *Chem Commun*, 2004, 1564–1579.
- V. Colombo, S. Galli, H. J. Choi, G. D. Han, A. Maspero, G. Palmisano, N. Masciocchi and J. R. Long, *Chem. Sci.*, 2011, **2**, 1311.
- M. Tonigold, Y. Lu, A. Mavrandonakis, A. Puls, R. Staudt, J. Möllmer, J. Sauer and D. Volkmer, *Chem. - Eur. J.*, 2011, **17**, 8671–8695.
- C. R. Wade, T. Corrales-Sanchez, T. C. Narayan and M. Dincă, *Energy Environ. Sci.*, 2013, **6**, 2172.
- L. He, L.-X. Cai, M.-H. Li, G.-L. Zhang, L.-P. Zhou, T. Chen, M.-J. Lin and Q.-F. Sun, *Chem. Sci.*, 2020, **11**, 7940–7949.
- R. K. Dubey, N. Westerveld, F. C. Grozema, E. J. R. Sudhölter and W. F. Jager, *Org. Lett.*, 2015, **17**, 1882–1885.
- N. Zink-Lorre, E. Font-Sanchis, Á. Sastre-Santos and F. Fernández-Lázaro, *Org. Chem. Front.*, 2017, **4**, 2016–2021.
- X. Lv, L. Zha, L. Qian, X. Xu, Q. Bi, Z. Xu, D. S. Wright and C. Zhang, *Chem. Eng. J.*, 2020, **386**, 123939.